Received July 30, 2015, accepted August 11, 2015, date of publication September 1, 2015, date of current version September 8, 2015.

Digital Object Identifier 10.1109/ACCESS.2015.2475237

Vector Perturbation Precoding for Multi-User CoMP Downlink Transmission

SANJEEWA P. HERATH, (Student Member, IEEE), DUY H. N. NGUYEN, (Member, IEEE), AND THO LE-NGOC, (Fellow, IEEE)

Department of Electrical and Computer Engineering, McGill University, Montréal, QC H3A 0E9, Canada

Corresponding author: S. P. Herath (sanjeewa.herath@mail.mcgill.ca)

This work was supported in part by the Natural Sciences and Engineering Research Council of Canada (NSERC) and in part by InterDigital Canada under an NSERC-Collaborative Research and Development (NSERC-CRD) grant.

ABSTRACT This paper focuses on the design of vector perturbation (VP) precoding for coordinated multi-point (CoMP) multi-user downlink transmission. Precoding is performed by individual base stations (BSs) in a distributed manner using only the downlink channel coefficients and user data local to a BS. A cascade precoder structure with an outer precoder managing the inter-cell interference (ICI) and an inner precoder performing mean-squared-error (MSE) minimization-based VP to mitigate the intra-cell interference is proposed. Three different outer precoding techniques are considered. In the first technique, the outer precoder is designed to fully eliminate the ICI by trading off the degrees of freedom (DoFs) available through multiple antennas. While the proposed technique outperforms existing conventional-VP based designs, a large portion of DoF is consumed by the ICI elimination. To overcome this issue, in the second technique, interference alignment-based outer precoding that minimizes the total leakage interference is proposed. To further improve the system performance, in the third approach, precoding by joint minimization of total leakage interference plus MSE is performed. Numerical results show that the proposed cascade precoding structure is an efficient way to use the DoF of CoMP multi-user downlink transmission.

INDEX TERMS MIMO broadcast channel, vector perturbation, non-linear precoding, multi-user MIMO, coordinated multipoint transmission.

I. INTRODUCTION

In a multi-cell downlink transmission, inter-cell interference (ICI) is a major impediment that deteriorates the performance of cell-edge users. To mitigate the impact of ICI or even take advantage of the inter-cell transmissions, coordinated multi-point (CoMP) has been considered as an effective technique [1]–[5]. When multi-antenna base stations (BSs) operate in CoMP transmission, the spatial degrees of freedom (DoF) can be utilized to manage the ICI and spatial division multiplexing enables intra-cell interference mitigation for multi-user communications [3]–[8].

Interference management in a downlink CoMP transmission can be implemented mainly by two schemes: i) joint processing (JP), and ii) coordinated precoding [1]–[4], [6], [9], [10]. In the JP technique, user data to all the serving users within the multi-cell system are simultaneously transmitted from all BSs such that the signals received from multiple BSs tend to reinforce constructively at the user receivers [3], [4], [9]–[12]. In this case, antennas from multiple BSs in the system act as one large transmit antenna array. The JP is feasible with backhaul connectivity among BSs to exchange channel coefficients and user data. However, due to the excessive backhaul demand for information exchange [3], [4], JP is less attractive in practical settings, but serves as a performance benchmark for comparison. On the other hand, in coordinated precoding, interference management with limited information exchange between BSs is focused [2]–[4], [13], [14]. As a result, backhaul overhead is reduced providing more attractive transmission techniques for realistic implementation.

It is noted that most of the previous works on CoMP in literature assumed linear precoding at each BS [9]–[11]. Recent works in [13] and [14] proposed multi-cell precoding schemes where non-linear dirty-paper coding (DPC) was utilized to enhance the CoMP system's sum-rate. This is because DPC is optimal for multiuser transmissions at each BS [15], [16]. However, DPC is prohibitively complex for practical implementation. Vector perturbation (VP) provides an alternative non-linear coding method that is capable of achieving near DPC performance with a reasonable

complexity [17], [18]. It has been shown that VP precoding outperforms linear precoding such as zero-forcing (ZF) and minimum mean-squared-error (MSE) in the single-cell environment [17]–[20]. Moreover, most of the additional computations for VP precoding is done at transmitter side [17]–[20]. For these reasons, VP precoding is promising for downlink multi-cell transmission with CoMP, but, to the best of our knowledge, the results are limited to [3] and [4].

In [3], assuming the user data and downlink channel coefficients to all serving users from all the BSs are available at a central processing unit, ZF based VP or so-called conventional-VP [19], [21]–[25] precoding has been applied under JP scheme. In conventional-VP precoding, the transmit signal is perturbed by a Gaussian integer vector (i.e., perturbation vector) for a given linear precoder such as ZF. The perturbation vector that has the smallest power scaling factor is used to suppress the noise enhancement effect [19], [21], [22]. To overcome the issue of high backhaul demand in [3], reference [4] focuses on coordinated VP precoding where only the downlink channel coefficients and user data local to a BS are needed. The major drawback of coordinated VP precoding proposed in [4] is that ZF based technique is applied to eliminate both ICI and inter-user interference. As a result, in [4], a large portion of DoF is consumed for ICI elimination and intra-cell users are served by conventional-VP precoding. Therefore, the precoder structure proposed in [4] fails to efficiently utilize the available DoF and to exploit the advantages offered by MSE minimization based VP precoding (or so-called MMSE-VP) [19]–[21], [26], [27]. Different from conventional-VP, the MMSE-VP precoding seeks a balance between noise enhancement suppression and residual interference mitigation [19]–[21], [26], [27] and thus, shown to outperform conventional-VP in single-cell environments [19]–[21], [26].

To overcome the aforementioned drawbacks of [3] and [4], we propose a cascade precoding structure for downlink CoMP transmission. The cascade precoder is devised with an outer precoder to coordinate the ICI and an inner precoder for the intra-cell interference management. The inner precoder exploits the advantages of MMSE-VP approach and hence boosts the performance of intra-cell multi-user transmission. Moreover, the cascade precoding is performed individually by each BS using only the channel coefficients and user data local to a BS. Therefore, the proposed cascade precoding structure provides design flexibility at a reduced backhaul overhead and computational complexity while efficiently using the available DoF to achieve a superior performance compared to [4].

We first look at the potential candidate techniques for outer precoder to fully eliminate the ICI. The objective is to trade-off the DoF available through multiple antennas to null the ICI such that the users in each cell experience an ICI-free transmission. Under this interference nulling (IN), we consider two approaches for outer precoder design based on QR factorization and singular-value decomposition (SVD) with different computational complexity. Then by using the remaining DoF, MMSE-VP based inner precoders, which match well to the ''effective channel'', are derived in closed-form. Bit-error-rate (BER) results show that the proposed precoders outperform the existing conventional-VP based technique in [4]. However, the major drawback of IN based outer precoding is that a larger portion of DoF is occupied by the ICI elimination. To relax this limitation and to explore other avenues for the ICI mitigation, we apply the idea of interference alignment (IA) for outer precoder where ''total interference leakage'' minimization approach [28], [29] is applied. However, a large gap between JP transmission benchmark performance and the proposed IN and IA techniques is still observed. To reduce this performance gap without increasing the backhaul information exchange compared to IN and IA, we next seek a balance between minimizing the interference leakage and the intra-cell MSE. First, the sum-MSE across multiple cells is decomposed into summations of the intra-cell MSE plus the total leakage to the other cells. This decomposition facilitates the sum-MSE minimization in a distributed manner by individual BSs. In particular, we derive a closed-form precoder that minimizes the total interference leakage plus the intra-cell MSE. The proposed precoder is shown to significantly outperform the existing design in [4] as well as the IN and IA methods.

We briefly summarize the notations used in this paper. Uppercase boldfaced letters are used to denote matrices and lowercase boldfaced letters for vectors. The superscripts $(\cdot)^{\top}$, $(\cdot)^{*}$, $(\cdot)^{\mathrm{H}}$ denote transpose, conjugate and conjugate transpose, respectively. diag$(\cdot)$ is a diagonal matrix where nonzero elements exist only on the main diagonal of the matrix. Tr$(\cdot)$ and Re$(\cdot)$ represent the trace and real value of an argument, respectively. $\|\cdot\|$ indicates the L_2-norm of a vector and $\mathbb{E}\{\cdot\}$ is the mathematical expectation. Moreover, $\jmath = \sqrt{-1}$ and $\mathbb{C}$ represents the set of all complex numbers while $\mathbb{Z}$ denotes the set of all integers. Notation $\mathcal{CN}(m, \sigma^2)$ denotes mean m and variance σ^2 circularly symmetric complex Gaussian (CSCG) random variable.

II. SYSTEM MODEL

Consider a multi-user MIMO CoMP downlink transmission consisting Q number of BSs. Each BS simultaneously serves K number of single-antenna users utilizing $M(\geq K)$ number of antennas. Each BS, say i^{th} one, constructs the symbol vector $\boldsymbol{d}_i = [d_{i1}, d_{i2}, \cdots, d_{iK}]^{\top} \in \mathbb{C}^{K\times 1}$ from i^{th} BS user data vector $\boldsymbol{u}_i = [u_{i1}, u_{i2}, \cdots, u_{iK}]^{\top} \in \mathbb{C}^{K\times 1}$ and perturbation vector $\boldsymbol{v}_i = [v_{i1}, v_{i2}, \cdots, v_{iK}]^{\top} \in \mathbb{C}^{K\times 1}$ such that

$$\boldsymbol{d}_i = \boldsymbol{u}_i + \tau \boldsymbol{v}_i \tag{1}$$

where τ is a positive scalar. The $\boldsymbol{v}_i$ is a complex Gaussian integer vector, i.e., v_{ij}, $j = 1, \cdots, K$ is a complex number in the set $\{a + \jmath b | a, b \in \mathbb{Z}\}$. More on τ and $\boldsymbol{v}$ will be discussed later in this section.

As shown in Fig. 1, we propose the cascade precoding structure for i^{th} BS where $\boldsymbol{W}_i$ and $\boldsymbol{G}_i$ represent the inner

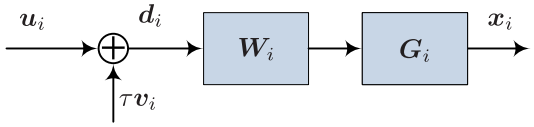

FIGURE 1. Cascade Precoding for Multi-Cell Multi-User Downlink.

and outer precoders, respectively. The symbol vector $\boldsymbol{d}_i$ is precoded by the i^{th} BS precoders to produce a precoded symbol vector $\boldsymbol{x}_i = [x_1, x_2, \cdots, x_M]^\top \in \mathbb{C}^{M\times 1}$, i.e.,

$$\boldsymbol{x}_i = \boldsymbol{G}_i \boldsymbol{W}_i \boldsymbol{d}_i. \tag{2}$$

Consequently, each user, say the j^{th} user served by the i^{th} BS receives the signal $y_{ij} \in \mathbb{C}$ over the channel $\boldsymbol{h}_{ij} \in \mathbb{C}^{M\times 1}$ contaminated by the additive white Gaussian noise (AWGN) $n_i \in \mathbb{C}$ and $n_i \sim \mathcal{CN}(0, N_0)$. The received signal of j^{th} user in i^{th} BS y_{ij} can be given by the compact form:

$$\boldsymbol{y}_i = \boldsymbol{H}_{ii}\boldsymbol{x}_i + \sum_{l=1, l\neq i}^{Q} \boldsymbol{H}_{li}\boldsymbol{x}_l + \boldsymbol{n}_i \tag{3}$$

where $\boldsymbol{y}_i = [y_{i1}, y_{i2}, \cdots, y_{iK}]^\top$, $\boldsymbol{H}_{li} = [\boldsymbol{h}_{l1}, \boldsymbol{h}_{l2}, \cdots, \boldsymbol{h}_{lK}]^{\text{H}}$ represents the channel matrix from l^{th} BS to the users served by i^{th} BS and $\boldsymbol{n}_i = [n_{i1}, n_{i2}, \cdots, n_{iK}]^\top$.

The τ is chosen to provide symmetric decoding regions around constellation points and the choice $\tau = 2(|c|_{\max} + \Delta/2)$, where $|c|_{\max}$ is the absolute value of the largest magnitude constellation symbol and Δ is the spacing between constellation points, serves this purpose [18]. With this choice for τ, each user is able to apply a modulo function $f_\tau(.)$ on the received signal independently (i.e., without cooperation among users) and remove v_i without knowing its value [18]. The function $f_\tau(.)$ is defined as

$$f_\tau(a) \triangleq a - \left\lfloor \frac{a + \tau/2}{\tau} \right\rfloor \tau \tag{4}$$

where $\lfloor . \rfloor$ denotes the largest integer less than or equal to its argument. Note that $f_\tau(.)$ is performed independently on both real and imaginary components of the received signal.

III. INTERFERENCE COORDINATION WITH VP

When a precoder designed for a single-cell environment is applied in a multi-cell environment, a poor performance is often observed due to ICI. Thus, it is reasonable to utilize the spatial DoF available through multiple antennas for complete ICI elimination or IN. In particular, we consider a multi-antenna BS in which a portion of DoF is utilized to fully eliminate the ICI and the remaining DoF are used to serve the intra-cell users. It means that a sufficiently large number of DoF is considered to be available. Note that these IN schemes need only channel state information (CSI) and user data local to the serving BS.

A. ZF BASED TECHNIQUE FOR INTERFERENCE COORDINATION

In [4], ZF based technique is applied to null the ICI. Particularly, it is assumed that the number of antennas at each BS is no less than the number of total serving users in the multi-cell system, i.e., $M \geq KQ$. In this case, [4] proposes to use conventional-VP with ZF precoder to simultaneously null the inter- and intra-cell interference. Then, a perturbation vector that minimizes the power scaling factor is used. For clarity, we next summarize this technique.

Scheme 1 (ZF Based ICI Nulling): Each BS, say i^{th} one, construct the $\boldsymbol{H}_i \in \mathbb{C}^{KQ\times M}$ using downlink channels local to i^{th} BS, i.e., $\boldsymbol{H}_{il}, l = 1, \cdots, Q$, where

$$\boldsymbol{H}_i = \left[\boldsymbol{H}_{i1}^\top \cdots \boldsymbol{H}_{iQ}^\top\right]^\top. \tag{5}$$

The pseudo-inverse of $\boldsymbol{H}_i$ can be written as

$$\hat{\boldsymbol{H}}_i = \boldsymbol{H}_i^{\text{H}}(\boldsymbol{H}_i\boldsymbol{H}_i^{\text{H}})^{-1} = \left[\hat{\boldsymbol{H}}_{i1} \cdots \hat{\boldsymbol{H}}_{iQ}\right] \in \mathbb{C}^{M\times KQ} \tag{6}$$

where $\hat{\boldsymbol{H}}_{ik} \in \mathbb{C}^{M\times K}, k = 1, \cdots, Q$. Thus we have

$$\boldsymbol{H}_{ik}\hat{\boldsymbol{H}}_{ik} = \begin{cases} \boldsymbol{I} & \text{if } i = k \\ \boldsymbol{0} & \text{if } i \neq k. \end{cases} \tag{7}$$

From (7), we observe that $\hat{\boldsymbol{H}}_{ii}$ can be used as the precoder for i^{th} BS to simultaneously eliminate both inter- and intra-cell interference. Thus the received signal of the j^{th} user served by the k^{th} BS can be written as

$$y_{jk} = \gamma_{i,\text{zf}}^{-1}\boldsymbol{d}_{i,\text{zf}} + \boldsymbol{n}_{jk} \tag{8}$$

where $\boldsymbol{d}_{i,\text{zf}} = \boldsymbol{u}_i + \tau\boldsymbol{v}_{i,\text{zf}}$. Here $\gamma_{i,\text{zf}}$ is the power scaling factor chosen to satisfy the BS power constraint P_i. The perturbation vector $\boldsymbol{v}_{i,\text{zf}}$ is found at i^{th} BS by

$$\boldsymbol{v}_{i,\text{zf}}^\star = \underset{\boldsymbol{v}_{i,\text{zf}}}{\text{minimize}} \ \|\hat{\boldsymbol{H}}_{ii}(\boldsymbol{u}_i + \tau\boldsymbol{v}_{i,\text{zf}})\|^2. \tag{9}$$

The optimization problem in (9) can efficiently be solved via sphere encoder algorithm similar to [18]–[20], [24], and [30] or reduced-complexity searching techniques developed in [19] and [31]. Note that only local CSI and user data are needed to perform precoding, i.e., i^{th} BS uses only $\boldsymbol{H}_{il}, l = 1, \cdots, Q$ and $\boldsymbol{u}_i$.

We observe from (7) and (8) that ZF based approach is applied for interference coordination. Moreover, a perturbation vector that minimizes the power scaling factor is used (cf. (9)). Hence, this IN scheme falls into the category of conventional-VP. To enhance the performance by exploiting the advantages offered by MMSE-VP technique, we propose MSE minimization based cascade precoding as follows.

B. CASCADE PRECODING FOR INTERFERENCE COORDINATION

In Scheme 1, using a conventional-VP based approach, interference-free transmission is provided for all the users in the system. However, the precoding structure in Scheme 1 fails to exploit the advantages offered by MMSE-VP for improved performance. To overcome this issue, we consider a cascade precoder of the form $\boldsymbol{G}_i\boldsymbol{W}_i$ for the i^{th} BS in which the outer precoder $\boldsymbol{G}_i$ manages the ICI while the inner precoder $\boldsymbol{W}_i$ performs the MMSE-VP on the "effective channel". Similar to Scheme 1, the proposed cascade precoding uses

only the local CSI and user data, i.e., $\boldsymbol{H}_{il}, l = 1, \cdots, Q$ and $\boldsymbol{u}_i$.

We first consider two techniques with varying computational complexity to perform outer precoding $\boldsymbol{G}_i$ that completely eliminates the ICI. The first method is based on the QR decomposition and the other one is based on SVD decomposition.

Scheme 2 (QR Decomposition Based ICI Nulling): First, $\boldsymbol{H}_i$ in (5) is constructed using local CSI and then, $\hat{\boldsymbol{H}}_{il}, l = 1, \cdots, Q$ in (6) is computed. Afterward, *reduced*-QR decomposition of $\hat{\boldsymbol{H}}_{ii} = \hat{\boldsymbol{Q}}_i\hat{\boldsymbol{R}}_i$ is performed where $\hat{\boldsymbol{Q}}_i \in \mathbb{C}^{M\times K}$ is a unitary matrix with $\hat{\boldsymbol{Q}}_i^{\mathrm{H}}\hat{\boldsymbol{Q}}_i = \boldsymbol{I}$ and $\hat{\boldsymbol{R}}_i \in \mathbb{C}^{K\times K}$ is an upper triangular matrix. From (7), we have

$$\boldsymbol{H}_{ik}\hat{\boldsymbol{H}}_{ii} = \boldsymbol{H}_{ik}\hat{\boldsymbol{Q}}_i\hat{\boldsymbol{R}}_i \overset{(a)}{=} \boldsymbol{H}_{ik}\hat{\boldsymbol{Q}}_i = \boldsymbol{0},\ i \neq k. \tag{10}$$

where (a) holds because the upper triangular matrix $\hat{\boldsymbol{R}}_i$ is invertible. Thus by choosing $\hat{\boldsymbol{Q}}_i$ as the outer precoder $\boldsymbol{G}_{i,\mathrm{qr}}$, ICI can be fully eliminated. As a result, given that no other-cell interference is affecting the intra-cell transmission, the input output relation of K users served by i^{th} BS can be written as

$$\boldsymbol{y}_{i,\mathrm{qr}} = \boldsymbol{H}_{ii}\hat{\boldsymbol{Q}}_i\boldsymbol{W}_{i,\mathrm{qr}}\boldsymbol{d}_{i,\mathrm{qr}} + \boldsymbol{n}_i \tag{11}$$

where $\boldsymbol{W}_{i,\mathrm{qr}}$ is the inner precoder to be designed to minimize the MSE between $\boldsymbol{d}_{i,\mathrm{qr}} = \boldsymbol{u}_i + \tau\boldsymbol{v}_{i,\mathrm{qr}}$ and $\hat{\boldsymbol{d}}_{i,\mathrm{qr}} \triangleq \gamma_{i,\mathrm{qr}}\boldsymbol{y}_{i,\mathrm{qr}}$. $\gamma_{i,\mathrm{qr}}$ is the power scaling factor chosen to satisfy the BS power constraint P_i. For this case, the searching for an optimal perturbation vector $\boldsymbol{v}_{i,\mathrm{qr}}$ will be discussed in Subsection III-C. The transmit signal power is $\|\hat{\boldsymbol{Q}}_i\boldsymbol{W}_{i,\mathrm{qr}}\boldsymbol{d}_{i,\mathrm{qr}}\|^2 = \|\boldsymbol{W}_{i,\mathrm{qr}}\boldsymbol{d}_{i,\mathrm{qr}}\|^2$ because $\hat{\boldsymbol{Q}}_i^{\mathrm{H}}\hat{\boldsymbol{Q}}_i = \boldsymbol{I}$.

The MSE minimization based VP precoding is performed over the effective channel. The effective channel of i^{th} BS, i.e., $\boldsymbol{H}_i^{(\mathrm{e,qr})} = \boldsymbol{H}_{ii}\hat{\boldsymbol{Q}}_i$ is

$$\boldsymbol{H}_i^{(\mathrm{e,qr})} = \boldsymbol{H}_{ii}\hat{\boldsymbol{Q}}_i\hat{\boldsymbol{R}}_i\hat{\boldsymbol{R}}_i^{-1} = \boldsymbol{H}_{ii}\hat{\boldsymbol{H}}_{ii}\hat{\boldsymbol{R}}_i^{-1} \overset{(b)}{=} \hat{\boldsymbol{R}}_i^{-1}. \tag{12}$$

Here (b) holds because, as given in (7), $\boldsymbol{H}_{ii}\hat{\boldsymbol{H}}_{ii} = \boldsymbol{I}$. Therefore, from (11), $\boldsymbol{y}_{i,\mathrm{qr}}$ can be written as

$$\boldsymbol{y}_{i,\mathrm{qr}} = \hat{\boldsymbol{R}}_i^{-1}\boldsymbol{W}_{i,\mathrm{qr}}\boldsymbol{d}_{i,\mathrm{qr}} + \boldsymbol{n}_i. \tag{13}$$

The relation in (13) will be used in Section III-C for inner precoder design.

Scheme 3 (SVD Decomposition Based ICI Nulling): Here, we focus on IN by a SVD decomposition based technique. Each BS, say i^{th} one, constructs the $\tilde{\boldsymbol{H}} \in \mathbb{C}^{K(Q-1)\times M}$ using CSI local to i^{th} BS where

$$\tilde{\boldsymbol{H}}_i = \left[\boldsymbol{H}_{i1}^{\top}, \cdots, \boldsymbol{H}_{i(i-1)}^{\top}, \boldsymbol{H}_{i(i+1)}^{\top}, \cdots, \boldsymbol{H}_{iQ}^{\top}\right]^{\top}. \tag{14}$$

To fully eliminate the ICI, $\boldsymbol{G}_{i,\mathrm{svd}} \in \mathbb{C}^{M\times r}$ is chosen in the right null-space of $\tilde{\boldsymbol{H}}$ by performing SVD decomposition of $\tilde{\boldsymbol{H}}_i$ where $r = \max(0, M - K(Q-1))$. In particular,

$$\tilde{\boldsymbol{H}}_i = \tilde{\boldsymbol{V}}_i\tilde{\boldsymbol{D}}_i[\tilde{\boldsymbol{U}}_{i,1}\ \tilde{\boldsymbol{U}}_{i,0}]^{\mathrm{H}} \tag{15}$$

where $\tilde{\boldsymbol{D}}_i$ is a diagonal matrix. $\tilde{\boldsymbol{V}}_i$ and $\tilde{\boldsymbol{U}}_i = [\tilde{\boldsymbol{U}}_{i,1}\tilde{\boldsymbol{U}}_{i,0}]^{\mathrm{H}} \in \mathbb{C}^{M\times M}$ represent the left- and right-singular vectors of $\tilde{\boldsymbol{H}}_i$. Note that to serve K intra-cell users, r needs to be no less than K. It means that similar to Schemes 1 and 2, $M \geq KQ$ should be satisfied. Moreover, $\tilde{\boldsymbol{U}}_{i,0} \in \mathbb{C}^{M\times(M-K(Q-1))}$ is in the null-space of $\boldsymbol{H}_{il}, l = 1, \cdots, Q, l \neq i$, i.e., $\boldsymbol{H}_{il}\tilde{\boldsymbol{U}}_{i,0} = \boldsymbol{0}$ which completely eliminates the ICI. Thus, the outer precoder $\boldsymbol{G}_{i,\mathrm{sv}}$ is chosen as $\tilde{\boldsymbol{U}}_{i,0}$. As a result, given that no other-cell interference is affecting the intra-cell transmission, the input output relation of K users served by i^{th} BS can be written as

$$\boldsymbol{y}_{i,\mathrm{sv}} = \boldsymbol{H}_{ii}\tilde{\boldsymbol{U}}_{i,0}\boldsymbol{W}_{i,\mathrm{sv}}\boldsymbol{d}_{i,\mathrm{sv}} + \boldsymbol{n}_i \tag{16}$$

where $\boldsymbol{W}_{i,\mathrm{sv}}$ is the inner precoder to be designed to minimize the MSE between $\boldsymbol{d}_{i,\mathrm{sv}} = \boldsymbol{u}_i + \tau\boldsymbol{v}_{i,\mathrm{sv}}$ and $\hat{\boldsymbol{d}}_{i,\mathrm{sv}} \triangleq \gamma_{i,\mathrm{sv}}\boldsymbol{y}_{i,\mathrm{sv}}$. The optimal perturbation vector $\boldsymbol{v}_{i,\mathrm{sv}}$ search will be discussed in Subsection III-C. $\gamma_{i,\mathrm{sv}}$ is the power scaling factor chosen to satisfy the BS power constraint P_i. In this case, the transmit signal power is $\|\tilde{\boldsymbol{U}}_{i,0}\boldsymbol{W}_{i,\mathrm{svd}}\boldsymbol{d}_{i,\mathrm{svd}}\|^2 = \|\boldsymbol{W}_i\boldsymbol{d}_{i,\mathrm{svd}}\|^2$ because $\tilde{\boldsymbol{U}}^{\mathrm{H}}_{i,0}\tilde{\boldsymbol{U}}_{i,0} = \boldsymbol{I}$. The effective channel of i^{th} BS $\boldsymbol{H}_i^{(\mathrm{e,sv})} = \boldsymbol{H}_{ii}\tilde{\boldsymbol{U}}_{i,0} \in \mathbb{C}^{K\times(M-K(Q-1))}$.

Scheme 4 (Interference Alignment Based ICI Mitigation): Observe that Schemes 1-3 need to satisfy $M \geq KQ$ and therefore, a larger portion of DoF is consumed for ICI cancellation. To address this issue, we next integrate the idea of IA [28], [29], [32], [33] for the outer precoder.

The K users in each BS experience the interference generated from the signals transmitted from other BSs, or so-called interference leakage [28], [29]. Our objective is to minimize the "total leakage interference" similar to [28] and [29] through the outer precoder. In particular, the focus is to precode the signal at transmitter i such that the coordinated interference at receiver l caused by transmitter i $(i \neq l)$ is minimum. The total interference leakage [28] can be written as

$$\mathcal{I}_{\mathrm{IA}} = \sum_{l=1}^{Q}\mathbb{E}\left\{\left\|\sum_{i=1,i\neq l}^{Q}\boldsymbol{H}_{il}\boldsymbol{G}_i\boldsymbol{x}_{i,\mathrm{ia}}\right\|^2\right\}. \tag{17}$$

where $\boldsymbol{x}_{i,\mathrm{ia}} \triangleq \boldsymbol{W}_{i,\mathrm{ia}}\boldsymbol{u}_i$. Taking the expectation of $\mathcal{I}_{\mathrm{IA}}$ in (17), we have

$$\mathcal{I}_{\mathrm{IA}} = \sum_{l=1}^{Q}\sum_{i=1,i\neq l}^{Q}\|\boldsymbol{H}_{il}\boldsymbol{G}_i\|^2 = \sum_{i=1}^{Q}\sum_{l=1,l\neq i}^{Q}\|\boldsymbol{H}_{il}\boldsymbol{G}_i\|^2. \tag{18}$$

By finding the lowest $\sum_{l=1,l\neq i}^{Q}\|\boldsymbol{H}_{il}\boldsymbol{G}_i\|^2$ over $\boldsymbol{G}_i$, individual BS can perform the minimization of $\mathcal{I}_{\mathrm{IA}}$ in a distributed manner. Similar to [28] and [29], we are interested in the semi-unitary precoder of the form $\boldsymbol{G}_i^{\mathrm{H}}\boldsymbol{G}_i = \boldsymbol{I}$. Thus, IA based optimal outer precoder, denoted as $\boldsymbol{G}_{i,\mathrm{ia}} \in \mathbb{C}^{M\times\lambda}$, can be given as:

$$\boldsymbol{G}_{i,\mathrm{ia}} = \nu_{\min}^{\lambda}\left(\sum_{l=1,l\neq i}^{Q}\boldsymbol{H}_{il}^{\mathrm{H}}\boldsymbol{H}_{il}\right) \tag{19}$$

where $\nu_{\min}^{\lambda}(\boldsymbol{X})$ is the matrix whose columns are the eigen-vectors corresponding to the λ smallest eigenvalues of matrix $\boldsymbol{X}$ [34, p. 45]. Here, $\lambda = \max(K, \pi)$ where π is the

TABLE 1. Cascade precoding for IN and IA techniques.

Scheme	Outer precoder $\boldsymbol{G}_{i,a}$	Inner precoder $\boldsymbol{W}_{i,a}$	Perturbation vector search: $\boldsymbol{\Psi}_{i,\mathrm{a}}$
2	$\hat{\boldsymbol{Q}}_i$	$\gamma_{i,\mathrm{qr}}^{-1}\hat{\boldsymbol{R}}_i\left(\frac{K}{\rho_i}\hat{\boldsymbol{R}}_i^{\mathrm{H}}\hat{\boldsymbol{R}}_i+\boldsymbol{I}\right)^{-1}$	$\hat{\boldsymbol{R}}_i^{\mathrm{H}}\hat{\boldsymbol{R}}_i\left(\hat{\boldsymbol{R}}_i^{\mathrm{H}}\hat{\boldsymbol{R}}_i+\frac{K}{\rho_i}\boldsymbol{I}\right)^{-1}$
3	$\tilde{\boldsymbol{U}}_{i,0}$	$\gamma_{i,\mathrm{sv}}^{-1}\tilde{\boldsymbol{U}}_{i,0}^{\mathrm{H}}\boldsymbol{H}_{ii}^{\mathrm{H}}\left(\boldsymbol{H}_{ii}\tilde{\boldsymbol{U}}_{i,0}\tilde{\boldsymbol{U}}_{i,0}^{\mathrm{H}}\boldsymbol{H}_{ii}^{\mathrm{H}}+\frac{K}{\rho_i}\boldsymbol{I}\right)^{-1}$	$\left(\boldsymbol{H}_{ii}\tilde{\boldsymbol{U}}_{i,0}\tilde{\boldsymbol{U}}_{i,0}^{\mathrm{H}}\boldsymbol{H}_{ii}^{\mathrm{H}}+\frac{K}{\rho_i}\boldsymbol{I}\right)^{-1}$
4	$\boldsymbol{G}_{i,\mathrm{ia}}$	$\gamma_{i,\mathrm{ia}}^{-1}\boldsymbol{G}_{i,\mathrm{ia}}^{\mathrm{H}}\boldsymbol{H}_{ii}^{\mathrm{H}}\left(\boldsymbol{H}_{ii}\boldsymbol{G}_{i,\mathrm{ia}}\boldsymbol{G}_{i,\mathrm{ia}}^{\mathrm{H}}\boldsymbol{H}_{ii}^{\mathrm{H}}+\frac{K}{\rho_i}\boldsymbol{I}\right)^{-1}$	$\left(\boldsymbol{H}_{ii}\boldsymbol{G}_{i,\mathrm{ia}}\boldsymbol{G}_{i,\mathrm{ia}}^{\mathrm{H}}\boldsymbol{H}_{ii}^{\mathrm{H}}+\frac{K}{\rho_i}\boldsymbol{I}\right)^{-1}$

nullity of $\sum_{l=1,l\neq i}^{Q}\boldsymbol{H}_{il}^{\mathrm{H}}\boldsymbol{H}_{il}$. The result in (19) indicates that the optimal precoder to minimize the total leakage lies in the smallest eigenvalue directions of $\sum_{l=1,l\neq i}^{Q}\boldsymbol{H}_{il}^{\mathrm{H}}\boldsymbol{H}_{il}$ and the condition $M \geq KQ$ may not be required. In this case, the effective channel to the users served by i^{th} BS is $\boldsymbol{H}_i^{(\mathrm{e,ia})} = \boldsymbol{H}_{ii}\boldsymbol{G}_{i,\mathrm{ia}}$. The transmit signal power is $\|\boldsymbol{G}_{i,\mathrm{ia}}\boldsymbol{W}_{i,\mathrm{ia}}\boldsymbol{d}_{i,\mathrm{ia}}\|^2 = \|\boldsymbol{W}_{i,\mathrm{ia}}\boldsymbol{d}_{i,\mathrm{ia}}\|^2$ because $\boldsymbol{G}_{i,\mathrm{ia}}^{\mathrm{H}}\boldsymbol{G}_{i,\mathrm{ia}} = \boldsymbol{I}$.

C. INNER MMSE-VP PRECODER DESIGN UNDER INTERFERENCE NULLING AND ALIGNMENT

The outer precoders proposed in Schemes 2-4 based on IN and IA coordinate the ICI. Next, we find the inner MMSE-VP precoder $\boldsymbol{W}_{i,\mathrm{a}}$ for Schemes 2-4 such that $\boldsymbol{x}_{i,\mathrm{a}} = \boldsymbol{W}_{i,\mathrm{a}}\boldsymbol{d}_{i,\mathrm{a}}$ where $\mathrm{a} \in \{\mathrm{sv, qr, ia}\}$. The scaled received signal $\hat{\boldsymbol{d}}_{i,\mathrm{a}}$, $\mathrm{a} \in \{\mathrm{sv, qr, ia}\}$ can be written as

$$\hat{\boldsymbol{d}}_{i,\mathrm{a}} = \gamma_{i,\mathrm{a}}\boldsymbol{H}_i^{(\mathrm{e,a})}\boldsymbol{x}_{i,\mathrm{a}} + \gamma_{i,\mathrm{a}}\boldsymbol{n}_i,\ \mathrm{a} \in \{\mathrm{sv, qr, ia}\} \tag{20}$$

where $\boldsymbol{H}_i^{(\mathrm{e,sv})} = \boldsymbol{H}_{ii}\tilde{\boldsymbol{U}}_{i,0}$, $\boldsymbol{H}_i^{(\mathrm{e,qr})} = \hat{\boldsymbol{R}}_i^{-1}$ and $\boldsymbol{H}_i^{(\mathrm{e,ia})} = \boldsymbol{H}_{ii}\boldsymbol{G}_{i,\mathrm{ia}}$. Furthermore, the transmit power constraint can be re-written as $\|\boldsymbol{x}_{i,\mathrm{a}}\|^2 = \|\boldsymbol{W}_{i,\mathrm{a}}\boldsymbol{d}_{i,\mathrm{a}}\|^2 \leq P_i$, $\mathrm{a} \in \{\mathrm{sv, qr, ia}\}$. The MSE between $\boldsymbol{d}_{i,\mathrm{a}}$ and $\hat{\boldsymbol{d}}_{i,\mathrm{a}}$ can be written as

$$\begin{aligned}\Xi_{i,\mathrm{a}} &= \mathbb{E}\left\{\|\gamma_{i,\mathrm{a}}\boldsymbol{H}_i^{(\mathrm{e,a})}\boldsymbol{x}_{i,\mathrm{a}} + \gamma_{i,\mathrm{a}}\boldsymbol{n}_i - \boldsymbol{d}_{i,\mathrm{a}}\|^2\right\}\\ &= \gamma_{i,\mathrm{a}}^2\boldsymbol{x}_{i,\mathrm{a}}^{\mathrm{H}}(\boldsymbol{H}_i^{(\mathrm{e,a})})^{\mathrm{H}}\boldsymbol{H}_i^{(\mathrm{e,a})}\boldsymbol{x}_{i,\mathrm{a}} - 2\gamma_{i,\mathrm{a}}\mathrm{Re}(\boldsymbol{d}_{i,\mathrm{a}}^{\mathrm{H}}\boldsymbol{H}_i^{(\mathrm{e,a})}\boldsymbol{x}_{i,\mathrm{a}})\\ &\quad + \gamma_{i,\mathrm{a}}^2 KN_0 + \boldsymbol{d}_{i,\mathrm{a}}^{\mathrm{H}}\boldsymbol{d}_{i,\mathrm{a}}.\end{aligned} \tag{21}$$

Thus, the precoding is performed by solving the following optimization problem:

$$\begin{aligned}&\underset{\boldsymbol{x}_{i,\mathrm{a}},\boldsymbol{v}_{i,\mathrm{a}},\gamma_{i,\mathrm{a}}}{\text{minimize}} \quad \Xi_{i,\mathrm{a}}\\ &\text{subject to} \quad \boldsymbol{x}_{i,\mathrm{a}}^{\mathrm{H}}\boldsymbol{x}_{i,\mathrm{a}} \leq P_i.\end{aligned} \tag{22}$$

Observe that the re-formulations in (22) can be solved similar to the single-cell MMSE-VP precoder design [20], [21], [26]. Therefore, for brevity in presentation, the details of the derivation are omitted. The inner precoders are derived in closed form and provided in Table 1. The perturbation vector search is found by performing Cholesky factorization of $\boldsymbol{\Psi}_{i,\mathrm{a}}$, $a \in \{\mathrm{sv, qr, ia}\}$ and given in Table 1. Note that $\rho_i \triangleq P_i/N_0$ denotes the signal-to-noise ratio (SNR) of the i^{th} BS. When deriving $\boldsymbol{W}_{i,\mathrm{qr}}$, the relation $(\boldsymbol{I} + \boldsymbol{A}^{-1})^{-1} = \boldsymbol{A}(\boldsymbol{I} + \boldsymbol{A})^{-1}$ [35, eq. (149)] is used for additional simplifications.

The overall operation of cascade precoding by IN and IA is given in Table 2. The optimal perturbation vector $\boldsymbol{v}_{i,a}^{\star}$ search can be done efficiently via sphere encoder algorithm [18]–[20], [24], [30], [31].

D. SUM-MSE MINIMIZATION

The IN technique (Schemes 2 and 3) fails when $M < KQ$. This issue is overcome by IA technique (Scheme 4) where precoding is performed to minimize the total leakage interference. However, illustrative numerical examples in Section V show that Schemes 2-4 have considerably large gaps compared to the JP benchmark. Therefore, to improve the system performance, we resort to the sum-MSE minimization approach. First, the sum-MSE is decomposed into intra-cell MSE plus total leakage interference. Using this result, precoding is performed with only CSI and user data local to a BS. The derived closed-form precoder is shown to outperform Schemes 2-4 in Section V through numerical results.

The received signal of all users served by i^{th} BS, i.e., $\boldsymbol{y}_i$ consists of the desired signal and the ICI from other cells as given in (3). The MSE between $\boldsymbol{y}_i$ and $\boldsymbol{d}_i$ of i^{th} BS denoted by MSE_i can be written as

$$\begin{aligned}\mathrm{MSE}_i &= \mathbb{E}\left\{\|\gamma\boldsymbol{y}_i - \boldsymbol{d}_i\|^2\right\}\\ &= \mathbb{E}\left\{\left\|\gamma\boldsymbol{H}_{ii}\boldsymbol{x}_i + \sum_{l=1,l\neq i}^{Q}\gamma\boldsymbol{H}_{li}\boldsymbol{x}_l + \gamma\boldsymbol{n}_i - \boldsymbol{d}_i\right\|^2\right\} \quad (23)\\ &= \sum_{l=1}^{Q}\gamma^2\boldsymbol{x}_l^{\mathrm{H}}\boldsymbol{H}_{li}^{\mathrm{H}}\boldsymbol{H}_{li}\boldsymbol{x}_l - 2\gamma\mathrm{Re}(\boldsymbol{x}_i^{\mathrm{H}}\boldsymbol{H}_{ii}^{\mathrm{H}}\boldsymbol{d}_i)\\ &\quad + \gamma^2 KN_0 + \boldsymbol{d}_i^{\mathrm{H}}\boldsymbol{d}_i \quad (24)\end{aligned}$$

where $\gamma > 0$ is a scaling factor. Therefore, the sum-MSE across all users in the multi-cell system, $\mathrm{MSE}_{\mathrm{sum}} = \sum_{i=1}^{Q}\mathrm{MSE}_i$ can be written as

$$\begin{aligned}\mathrm{MSE}_{\mathrm{sum}} &= \sum_{i=1}^{Q}\left(\sum_{l=1}^{Q}\gamma^2\boldsymbol{x}_l^{\mathrm{H}}\boldsymbol{H}_{li}^{\mathrm{H}}\boldsymbol{H}_{li}\boldsymbol{x}_l - 2\gamma\mathrm{Re}(\boldsymbol{x}_i^{\mathrm{H}}\boldsymbol{H}_{ii}^{\mathrm{H}}\boldsymbol{d}_i)\right.\\ &\qquad \left.+\gamma^2 KN_0 + \boldsymbol{d}_i^{\mathrm{H}}\boldsymbol{d}_i\right)\\ &= \sum_{i=1}^{Q}\left(\|\gamma\boldsymbol{H}_{li}\boldsymbol{x}_l - \boldsymbol{d}_i\|^2 + \gamma^2 KN_0\right.\\ &\qquad \left.+\sum_{l=1,l\neq i}^{Q}\|\gamma\boldsymbol{H}_{li}\boldsymbol{x}_l\|^2\right).\end{aligned}$$

TABLE 2. Cascade precoding by IN & IA techniques (schemes 2, 3 & 4).

Input	$\boldsymbol{u}_i$, and $\boldsymbol{H}_{il}, l = 1, \cdots, Q$
Output	$\boldsymbol{W}_{i,a}$, $\boldsymbol{G}_{i,a}$ $\gamma_{i,a}$, $\boldsymbol{v}^{\star}_{i,a}$, $a \in \{\text{sv, qr, ia}\}$
	Scheme 2: Construct $\boldsymbol{H}_i = \left[\boldsymbol{H}_{i1}^{\top} \cdots \boldsymbol{H}_{iQ}^{\top}\right]^{\top}$ & find the pseudo inverse of $\boldsymbol{H}_i$ by $\hat{\boldsymbol{H}}_i = \boldsymbol{H}_i^{\mathrm{H}}(\boldsymbol{H}_i\boldsymbol{H}_i^{\mathrm{H}})^{-1}$ $= \left[\hat{\boldsymbol{H}}_{i1} \cdots \hat{\boldsymbol{H}}_{iQ}\right]$. Perform QR of $\hat{\boldsymbol{H}}_{ii}$ to find $\hat{\boldsymbol{R}}_i$ & $\boldsymbol{G}_{i,\text{qr}} = \hat{\boldsymbol{Q}}_i$
Step i	**Scheme 3**: Construct $\tilde{\boldsymbol{H}}_i = \left[\boldsymbol{H}_{i1}^{\top}, \cdots, \boldsymbol{H}_{i(i-1)}^{\top}, \boldsymbol{H}_{i(i+1)}^{\top}, \cdots, \boldsymbol{H}_{iQ}^{\top}\right]^{\top}$ & perform SVD decomposition of $\tilde{\boldsymbol{H}}_i = \tilde{\boldsymbol{V}}_i\tilde{\boldsymbol{D}}_i[\tilde{\boldsymbol{U}}_{i,1}\tilde{\boldsymbol{U}}_{i,0}]^{\mathrm{H}}$ to find $\boldsymbol{G}_{i,\text{svd}} = \tilde{\boldsymbol{U}}_{i,0}$
	Scheme 4: Construct $\sum_{l=1,l\neq i}^{Q} \boldsymbol{H}_{il}^{\mathrm{H}}\boldsymbol{H}_{il}$ & perform SVD decomposition. Choose the eigenvectors correspond to the $\lambda = \max(K, \pi)$ smallest eigenvalues as $\boldsymbol{G}_{i,\text{ia}}$
Step ii	Perform Cholesky decomposition & find $\boldsymbol{L}_{i,a}$ such that $\boldsymbol{\Psi}_{i,a} = \boldsymbol{L}_{i,a}^{\mathrm{H}}\boldsymbol{L}_{i,a}$ where $\boldsymbol{\Psi}_{i,a}$ is given in Table I
Step iii	Find $\boldsymbol{v}^{\star}_{i,a}$ by solving $\boldsymbol{v}^{\star}_{i,a} = \underset{\boldsymbol{v}_{i,a}}{\text{minimize}} \left\|\boldsymbol{L}_{i,a}(\boldsymbol{u}_i + \tau\boldsymbol{v}_{i,a})\right\|^2$
Step iv	Compute $\boldsymbol{d}_{i,a} = \boldsymbol{u}_i + \tau\boldsymbol{v}^{\star}_{i,a}$,
	Scheme 2: $\boldsymbol{W}_{i,\text{qr}} = \gamma_{i,\text{qr}}^{-1}\hat{\boldsymbol{R}}_i(\frac{K}{\rho_i}\hat{\boldsymbol{R}}_i^{\mathrm{H}}\hat{\boldsymbol{R}}_i + \boldsymbol{I})^{-1}$
	Scheme 3: $\boldsymbol{W}_{i,\text{sv}} = \gamma_{i,\text{sv}}^{-1}\tilde{\boldsymbol{U}}_{i,0}^{\mathrm{H}}\boldsymbol{H}_{ii}^{\mathrm{H}}(\boldsymbol{H}_{ii}\tilde{\boldsymbol{U}}_{i,0}\tilde{\boldsymbol{U}}_{i,0}^{\mathrm{H}}\boldsymbol{H}_{ii}^{\mathrm{H}} + \frac{K}{\rho_i}\boldsymbol{I})^{-1}$
	Scheme 4: $\boldsymbol{W}_{i,\text{ia}} = \gamma_{i,\text{ia}}^{-1}\boldsymbol{G}_{i,\text{ia}}^{\mathrm{H}}\boldsymbol{H}_{ii}^{\mathrm{H}}(\boldsymbol{H}_{ii}\boldsymbol{G}_{i,\text{ia}}\boldsymbol{G}_{i,\text{ia}}^{\mathrm{H}}\boldsymbol{H}_{ii}^{\mathrm{H}} + \frac{K}{\rho_i}\boldsymbol{I})^{-1}$

Since $\sum_{i=1}^{Q}\sum_{l=1,l\neq i}^{Q}\|\boldsymbol{H}_{li}\boldsymbol{x}_l\|^2 = \sum_{i=1}^{Q}\sum_{l=1,l\neq i}^{Q}\|\boldsymbol{H}_{il}\boldsymbol{x}_i\|^2$, MSE_{sum} can be written as $\text{MSE}_{\text{sum}} = \sum_{i=1}^{Q}\tilde{\Psi}_i$ where

$$\begin{aligned}\tilde{\Psi}_i &= \|\gamma\boldsymbol{H}_{li}\boldsymbol{x}_l - \boldsymbol{d}_i\|^2 + \gamma^2 KN_0 + \sum_{l=1,l\neq i}^{Q}\|\gamma\boldsymbol{H}_{li}\boldsymbol{x}_l\|^2 \\ &= \mathbb{E}\left\{\|\gamma\boldsymbol{H}_{ii}\boldsymbol{x}_i + \gamma\boldsymbol{n}_i - \boldsymbol{d}_i\|^2\right\} + \sum_{l=1,l\neq i}^{Q}\|\gamma\boldsymbol{H}_{il}\boldsymbol{x}_i\|^2 \quad (25)\end{aligned}$$

Here (25) holds because $\boldsymbol{n}_i$ is independent of $\boldsymbol{H}_{ii}$, $\mathbb{E}\{\boldsymbol{n}_i\} = \boldsymbol{0}$ and $\mathbb{E}\{\boldsymbol{n}_i^{\mathrm{H}}\boldsymbol{n}_i\} = KN_0$.

In (25), the first term represents the intra-cell MSE of i^{th} BS while the second term represents the total interference leakage from i^{th} BS to all the other users of other cells [36]. Observe that $\tilde{\Psi}_i$ depends only on the CSI and user data local to i^{th} BS, i.e., $\boldsymbol{H}_{il}$, $l = 1, \cdots, Q$ and $\boldsymbol{u}_i$. To facilitate distributed processing and to obtain the precoder in closed-form while simplifying the analysis, similar to [11], [19], [20], [27], and [36], we modify $\tilde{\Psi}_i$ in (25). The modified MSE of i^{th} BS denoted by Ψ_i is written as

$$\begin{aligned}\Psi_i &= \sum_{i=1}^{Q}\mathbb{E}\left\{\|\gamma_i\boldsymbol{H}_{ii}\boldsymbol{x}_i + \gamma_i\boldsymbol{n}_i - \boldsymbol{d}_i\|^2 + \sum_{l=1,l\neq i}^{Q}\|\gamma_i\boldsymbol{H}_{il}\boldsymbol{x}_i\|^2\right\} \\ &= \sum_{l=1}^{Q}\gamma_i^2\boldsymbol{x}_i^{\mathrm{H}}\boldsymbol{H}_{il}^{\mathrm{H}}\boldsymbol{H}_{il}\boldsymbol{x}_i - 2\gamma_i\text{Re}(\boldsymbol{x}_i^{\mathrm{H}}\boldsymbol{H}_{ii}^{\mathrm{H}}\boldsymbol{d}_i) + \gamma_i^2 KN_0 + \boldsymbol{d}_i^{\mathrm{H}}\boldsymbol{d}_i \quad (26)\end{aligned}$$

Observe that the minimization of Ψ_i in (26) can be done by each BS individually knowing only local CSI and user data which is the same that needed in IN and IA techniques. Thus, the i^{th} BS performs precoding to minimize Ψ_i where $\boldsymbol{x}_i = \boldsymbol{W}_{i,\text{mse}}\boldsymbol{d}_i$. Note that this precoder design is a special case of cascade precoding with $\boldsymbol{G}_i = \boldsymbol{I}$.

Scheme 5 (Total Leakage Interference Plus MSE Minimization Based VP Precoding): The objective is to find the VP precoder that minimizes Ψ_i by i^{th} BS. Therefore, i^{th} BS has following optimization problem:

$$\begin{aligned}&\underset{\boldsymbol{x}_i,\boldsymbol{v}_i,\gamma_i}{\text{minimize}} \quad \Psi_i \\ &\text{subject to} \quad \boldsymbol{x}_i^{\mathrm{H}}\boldsymbol{x}_i \leq P_i. \quad (27)\end{aligned}$$

Note that $\boldsymbol{x}_i$ and γ_i are continuous variables and $\boldsymbol{v}_i$ is a discrete variable. We first minimize Ψ_i with respect to $\boldsymbol{x}_i$ and γ_i for a given $\boldsymbol{v}_i$ using the Lagrangian approach. Then, by substituting the obtained results for $\boldsymbol{x}_i$ and γ_i, the minimization with respect to $\boldsymbol{v}_i$ is carried out.

The Lagrangian for the optimization problem in (27) can be written as

$$\Lambda_2(\boldsymbol{x}_i, \boldsymbol{v}_i, \gamma_i) = \Psi_i + \mu(\boldsymbol{x}_i^{\mathrm{H}}\boldsymbol{x}_i - P_i) \quad (28)$$

where μ is the Lagrangian multiplier. By applying the Karush-Kuhn-Tucker (KKT) conditions, we find the solutions of continuous variables $\boldsymbol{x}_i$ and γ_i for a fixed $\boldsymbol{d}_i$ (i.e., for a given $\boldsymbol{v}_i$). From the stationarity of the Lagrangian, we have

$$\frac{\partial\Lambda_2}{\partial\boldsymbol{x}_i} = \sum_{l=1}^{Q}\gamma_i^2\boldsymbol{H}_{il}^{\top}\boldsymbol{H}_{il}^{*}\boldsymbol{x}_i^{*} - \gamma_i\boldsymbol{H}_{ii}^{\top}\boldsymbol{d}^{*} + \mu\boldsymbol{x}_i^{*} = \boldsymbol{0}, \quad (29a)$$

$$\frac{\partial\Lambda_2}{\partial\gamma_i} = \sum_{l=1}^{Q}\gamma_i\boldsymbol{x}_i^{\mathrm{H}}\boldsymbol{H}_{il}^{\mathrm{H}}\boldsymbol{H}_{il}\boldsymbol{x}_i - \text{Re}\left(\boldsymbol{d}_i^{\mathrm{H}}\boldsymbol{H}_{ii}\boldsymbol{x}_i\right) + \gamma_i KN_0 = 0. \quad (29b)$$

TABLE 3. Operation of total leakage interference plus MSE minimization based VP precoding.

Input	$\boldsymbol{u}_i$ & $\boldsymbol{H}_{il}, l = 1, \cdots, Q$
Output	$\boldsymbol{W}_{i,\text{mse}}$, γ_i, $\boldsymbol{v}_i^\star$
Step i	Perform Cholesky decomposition of $\boldsymbol{\Theta}_i = \boldsymbol{I} - \boldsymbol{H}_{ii}\left[\sum_{i=1}^{Q}\boldsymbol{H}_{il}^{\text{H}}\boldsymbol{H}_{il} + \frac{K}{\rho_i}\boldsymbol{I}\right]^{-1}\boldsymbol{H}_{ii}^{\text{H}}$ & find $\boldsymbol{L}_{i,\text{mse}}$ such that $\boldsymbol{\Theta}_i = \boldsymbol{L}_{i,\text{mse}}^{\text{H}}\boldsymbol{L}_{i,\text{mse}}$
Step ii	Find $\boldsymbol{v}_i^\star$ by solving $\boldsymbol{v}_i^\star = \underset{\boldsymbol{v}_i}{\text{minimize}}\ \|\boldsymbol{L}_{i,\text{mse}}(\boldsymbol{u}_i + \tau\boldsymbol{v}_i)\|^2$
Step iii	Compute $\boldsymbol{d}_i = \boldsymbol{u}_i + \tau\boldsymbol{v}_i^\star$, $\gamma_i = \sqrt{\frac{1}{P_i}\boldsymbol{d}_i^{\text{H}}\boldsymbol{H}_{ii}\left(\sum_{l=1}^{Q}\boldsymbol{H}_{il}^{\text{H}}\boldsymbol{H}_{il} + \frac{K}{\rho_i}\boldsymbol{I}\right)^{-2}\boldsymbol{H}_{ii}^{\text{H}}\boldsymbol{d}_i}$, $\boldsymbol{W}_{i,\text{mse}} = \frac{1}{\gamma_i}\left(\sum_{l=1}^{Q}\boldsymbol{H}_{il}^{\text{H}}\boldsymbol{H}_{il} + \frac{K}{\rho_i}\boldsymbol{I}\right)^{-1}\boldsymbol{H}_{ii}^{\text{H}}$.

Taking the transpose of (29a) and multiplying it by $\boldsymbol{x}_i/\gamma_i$, we arrive at

$$\sum_{l=1}^{Q}\gamma_i\boldsymbol{x}_i^{\text{H}}\boldsymbol{H}_{il}^{\text{H}}\boldsymbol{H}_{il}\boldsymbol{x}_i - \boldsymbol{d}_i^{\text{H}}\boldsymbol{H}_{ii}\boldsymbol{x}_i + \frac{\mu}{\gamma_i}\boldsymbol{x}_i^{\text{H}}\boldsymbol{x}_i = 0. \tag{30}$$

Observe that $\boldsymbol{d}_i^{\text{H}}\boldsymbol{H}_{ii}\boldsymbol{x}_i$ is real-valued and therefore, from (29b) and (30) we have

$$\mu\boldsymbol{x}_i^{\text{H}}\boldsymbol{x}_i = \gamma_i^2 KN_0.$$

If $\boldsymbol{x}_i = \boldsymbol{0}$, then we have $\gamma_i = 0$, which is a contradiction. Hence, $\boldsymbol{x}_i \neq \boldsymbol{0}$ and therefore, $\mu = \frac{\gamma_i^2 KN_0}{\boldsymbol{x}_i^{\text{H}}\boldsymbol{x}_i} > 0$. Moreover, from complementary slackness, it is necessary that $\mu(\boldsymbol{x}_i^{\text{H}}\boldsymbol{x}_i - P_i) = 0$. Since $\mu > 0$, we have $\boldsymbol{x}_i^{\text{H}}\boldsymbol{x}_i = P_i$. Therefore, $\mu = \gamma_i^2 KN_0/P_i$. Thus, by taking the transpose of (29a), we arrive at

$$\sum_{l=1}^{Q}\gamma_i^2\boldsymbol{x}_i^{\text{H}}\boldsymbol{H}_{il}^{\text{H}}\boldsymbol{H}_{il} - \gamma_i\boldsymbol{d}_i^{\text{H}}\boldsymbol{H}_{ii} + \frac{1}{P_i}\gamma_i^2 KN_0\boldsymbol{x}_i^{\text{H}} = \boldsymbol{0}.$$

Hence, from (2) we have

$$\boldsymbol{W}_{i,\text{mse}} = \frac{1}{\gamma_i}\left(\sum_{l=1}^{Q}\boldsymbol{H}_{il}^{\text{H}}\boldsymbol{H}_{il} + \frac{K}{\rho_i}\boldsymbol{I}\right)^{-1}\boldsymbol{H}_{ii}^{\text{H}} \tag{31}$$

where (31) is obtained using the relation $\boldsymbol{x}_i^{\text{H}}\boldsymbol{x}_i = P_i$ and

$$\gamma_i = \sqrt{\frac{1}{P_i}\boldsymbol{d}_i^{\text{H}}\boldsymbol{H}_{ii}\left(\sum_{l=1}^{Q}\boldsymbol{H}_{il}^{\text{H}}\boldsymbol{H}_{il} + \frac{1}{P_i}KN_0\boldsymbol{I}\right)^{-2}\boldsymbol{H}_{ii}^{\text{H}}\boldsymbol{d}_i}. \tag{32}$$

Next, Ψ_i in (26) is minimized over $\boldsymbol{v}_i$ for obtained $\boldsymbol{x}_i$ and γ_i in (31) and (32), respectively. As $\boldsymbol{x}_i$ and γ_i satisfy (29b), from (26), the simplified Ψ_i can be written as

$$\begin{aligned}\Psi_i &= \boldsymbol{d}_i^{\text{H}}\left\{\boldsymbol{I} - \boldsymbol{H}_{ii}\left(\sum_{l=1}^{Q}\boldsymbol{H}_{il}^{\text{H}}\boldsymbol{H}_{il} + \frac{1}{P_i}KN_0\boldsymbol{I}\right)^{-1}\boldsymbol{H}_{ii}^{\text{H}}\right\}\boldsymbol{d}_i \\ &= \boldsymbol{d}_i^{\text{H}}\boldsymbol{\Theta}_i\boldsymbol{d}_i \end{aligned} \tag{33}$$

where $\boldsymbol{\Theta}_i = \boldsymbol{I} - \boldsymbol{H}_{ii}\left[\sum_{i=1}^{Q}\boldsymbol{H}_{il}^{\text{H}}\boldsymbol{H}_{il} + \frac{K}{\rho_i}\boldsymbol{I}\right]^{-1}\boldsymbol{H}_{ii}^{\text{H}}$. By applying the Cholesky decomposition to $\boldsymbol{\Theta}_i$, i.e., $\boldsymbol{\Theta}_i = L_{i,\text{mse}}^{\text{H}}\boldsymbol{L}_{i,\text{mse}}$, the optimization problem to find the optimal $\boldsymbol{v}_i$ can be re-formulated as an integer lattice least square problem:

$$\boldsymbol{v}_i^\star = \underset{\boldsymbol{v}_i}{\text{minimize}}\|\boldsymbol{L}_{i,\text{mse}}(\boldsymbol{u}_i + \tau\boldsymbol{v}_i)\|^2. \tag{34}$$

The optimization problem in (34) can efficiently be solved via sphere encoder algorithm similar to [18]–[20], [24], and [30] or reduced-complexity searching techniques developed in [19] and [31]. The overall operation of the proposed multi-cell precoding design is summarized in Table 3.

E. COMPUTATIONAL COMPLEXITY

While all users perform modulo operation in (4) before demodulation, we observe that IN, IA and total interference leakage plus intra-cell MSE minimization based precoding schemes have different computational complexity at the BS.

In Scheme 1 proposed in [4] where ZF based ICI nulling, matrix inversion to calculate $\hat{\boldsymbol{H}}_i$ and perturbation vector search in (9) by sphere encoding to find $\boldsymbol{v}_{i,\text{zf}}^\star$ are the major computational intensive operations. Computational complexity of cascade precoding with IN and IA can be computed from Table 2. In Scheme 2 with QR factorization, the outer precoder $\boldsymbol{G}_{i,\text{qr}}$ is obtained by a matrix inversion to calculate $\hat{\boldsymbol{H}}_i$, QR factorization of $\hat{\boldsymbol{H}}_{ii}$. The perturbation vector $\boldsymbol{v}_{i,\text{qr}}^\star$ is found by computing $\boldsymbol{\Psi}_{i,\text{qr}}$ which involves a matrix inversion (to compute $\boldsymbol{\Psi}_{i,\text{qr}}$) and Cholesky factorization (to compute $\boldsymbol{L}_{i,\text{qr}}$) and sphere encoding (to find $\boldsymbol{v}_{i,\text{qr}}^\star$). Note that, an additional matrix inversion is not necessary to compute the inner precoder $\boldsymbol{W}_{i,\text{qr}}$ as the matrix inversion performed to find $\boldsymbol{\Psi}_{i,\text{qr}}$ can be reused. On the other hand, in Scheme 3, SVD decomposition is necessary to find outer precoder $\boldsymbol{G}_{i,\text{sv}}$. The computational complexity to find inner precoder $\boldsymbol{W}_{i,\text{sv}}$ and perturbation vector $\boldsymbol{v}_{i,\text{sv}}$ is the same that of Scheme 2. As shown in Table 3, in Scheme 5, a channel inversion operation is necessary to compute $\boldsymbol{\Theta}_i$, Cholesky factorization to find $\boldsymbol{L}_{i,\text{mse}}$ and sphere encoding to obtain $\boldsymbol{v}_i^\star$.

TABLE 4. Computational complexity in flops.

Scheme	Computation of Precoders ($\boldsymbol{W}_{i,\mathrm{a}}$ & $\boldsymbol{G}_{i,\mathrm{a}}$)	Computing optimal perturbation vector ($\boldsymbol{v}_{i,a}^{\star}$)
1	• Inverse of $\boldsymbol{H}_i\boldsymbol{H}_i^{\mathrm{H}} \in \mathbb{C}^{KQ\times KQ}$ to compute $\hat{\boldsymbol{H}}_i$: $\frac{7}{3}(KQ)^3$ flops	• Sphere encoder
2	• Inverse of $\boldsymbol{H}_i\boldsymbol{H}_i^{\mathrm{H}} \in \mathbb{C}^{KQ\times KQ}$ to compute $\hat{\boldsymbol{H}}_i$: $\frac{7}{3}(KQ)^3$ flops • QR factorization of $\hat{\boldsymbol{H}}_{ii} \in \mathbb{C}^{M\times K}$: $2MK^2$ flops	• Inverse of $(\boldsymbol{H}_{ii}\boldsymbol{H}_{ii}^{\mathrm{H}} + \rho_i\boldsymbol{I})^{-1} \in \mathbb{C}^{K\times K}$ to find $\boldsymbol{\Psi}_{i,a}$: $\frac{7}{3}K^3$ flops • Cholesky factorization of $\boldsymbol{\Psi}_{i,a}$: $\frac{1}{3}K^3$ flops • Sphere encoder
3	• SVD decomposition of $\tilde{\boldsymbol{H}} \in \mathbb{C}^{K(Q-1)\times M}$: $2K(Q-1)M^2 + 11M^3$ flops	• Same complexity as perturbation vector search of Scheme 2
4	• SVD decomposition of $\sum_{l=1,l\neq i}^{Q} \boldsymbol{H}_{il}^{\mathrm{H}}\boldsymbol{H}_{il} \in \mathbb{C}^{M\times M}$: $13M^3$ flops	• Same complexity as perturbation vector search of Scheme 2
5	• Inverse of $\sum_{i=1}^{Q} \boldsymbol{H}_{il}^{\mathrm{H}}\boldsymbol{H}_{il} + \frac{K}{\rho_i}\boldsymbol{I}$ $\in \mathbb{C}^{M\times M}$: $\frac{7}{3}M^3$ flops	• Cholesky factorization of $\boldsymbol{\Theta}_i$: $\frac{1}{3}K^3$ flops • Sphere encoder

The computational complexity of these main operations in terms of flops is shown in Table 4. Note that same dimensional sphere encoder is used in all the schemes and hence a fair comparison can be done without counting its computational complexity. We consider a computational complexity of a system where 3 BSs ($Q = 3$) each having 12 transmit antennas ($M = 12$) and each BS serving 4 users ($K = 4$). Observe that the parameter values satisfy $M = KQ$ and therefore, Schemes 1-5 are feasible. For the selected parameter values, the complexity to compute $\boldsymbol{W}_{i,\mathrm{a}}$ of Schemes 1-5 is 4032, 4458, 6827, 6656 and 1216 flops, respectively. The computation of optimal perturbation vector is the lowest in Scheme 1 while additional 21 flop count is needed for Scheme 5 and additional 170 flop count is needed for Schemes 2-4.

IV. JOINT PROCESSING

Here, the JP is considered as a benchmark performance criterion to compare the interference coordination schemes in Section III. We assume that a central node has all downlink channel coefficients (i.e., $\boldsymbol{H}_{il}, i = 1,\cdots,Q, l = 1,\cdots,Q$) and all user data (i.e., $\boldsymbol{u}_i, i = 1,\cdots,Q$) through a backhaul link. To perform JP MMSE-VP precoding for CoMP downlink, the input and output relationship is reformulated as follows.

The received signal of all users in the multi-cell system $\boldsymbol{y} = (\boldsymbol{y}_1, \boldsymbol{y}_2, \cdots, \boldsymbol{y}_Q)^{\top}$ can be written as

$$\boldsymbol{y} = \boldsymbol{H}\boldsymbol{x} + \boldsymbol{n} \tag{35}$$

where $\boldsymbol{x} = (\boldsymbol{x}_1, \boldsymbol{x}_2, \cdots, \boldsymbol{x}_Q)^{\top}$, $\boldsymbol{n} = (\boldsymbol{n}_1, \boldsymbol{n}_2, \cdots, \boldsymbol{n}_Q)^{\top}$ and

$$\boldsymbol{H} = \begin{pmatrix} \boldsymbol{H}_{11} & \boldsymbol{H}_{21} & \cdots & \boldsymbol{H}_{Q1} \\ \boldsymbol{H}_{12} & \boldsymbol{H}_{22} & \cdots & \boldsymbol{H}_{Q2} \\ \vdots & \vdots & \cdots & \vdots \\ \boldsymbol{H}_{1Q} & \boldsymbol{H}_{2Q} & \cdots & \boldsymbol{H}_{QQ} \end{pmatrix}. \tag{36}$$

Here $\boldsymbol{x} = \boldsymbol{d} + \tau\boldsymbol{v}$ where $\boldsymbol{d} = (\boldsymbol{d}_1, \boldsymbol{d}_2, \cdots, \boldsymbol{d}_Q)^{\top}$ and $\boldsymbol{v} = (\boldsymbol{v}_1, \boldsymbol{v}_2, \cdots, \boldsymbol{v}_Q)^{\top}$. Each user scale y_{ij} by the power normalization factor to produce the scaled received signal $\hat{\boldsymbol{d}} \triangleq \gamma\boldsymbol{y}$. We have chosen $\gamma > 0$ to satisfy the BS power constraints [18]–[20], [27]. The MSE between $\boldsymbol{d}$ and $\hat{\boldsymbol{d}}$ can be derived as

$$\begin{aligned} \Xi(\boldsymbol{x},\boldsymbol{v},\gamma) &= \mathbb{E}\left\{\|\gamma\boldsymbol{H}\boldsymbol{x} + \gamma\boldsymbol{n} - \boldsymbol{d}\|^2\right\} \\ &= \gamma^2\boldsymbol{x}^{\mathrm{H}}\boldsymbol{H}^{\mathrm{H}}\boldsymbol{H}\boldsymbol{x} - 2\gamma\mathrm{Re}\left(\boldsymbol{d}^{\mathrm{H}}\boldsymbol{H}\boldsymbol{x}\right) + \gamma^2 KQN_0 \\ &\quad + \boldsymbol{d}^{\mathrm{H}}\boldsymbol{d} \\ &= \|\gamma\boldsymbol{H}\boldsymbol{x} - \boldsymbol{d}\|^2 + \gamma^2 KQN_0 \end{aligned} \tag{37}$$

The optimization problem to find the precoder with individual BS power constraint can therefore be written as

$$\begin{aligned} &\underset{\boldsymbol{x},\boldsymbol{v},\gamma}{\text{minimize}} \quad \Xi(\boldsymbol{x},\boldsymbol{v},\gamma) \\ &\text{subject to} \quad \boldsymbol{x}^{\mathrm{H}}\Pi_i^{\mathrm{H}}\boldsymbol{\Pi}_i\boldsymbol{x} \leq P_i, i = 1,2,\cdots,Q \end{aligned} \tag{38}$$

where $\boldsymbol{\Pi}_i = \mathrm{diag}(\boldsymbol{0}_{(i-1)M}, \boldsymbol{1}_M, \boldsymbol{0}_{(Q-i)M})$, P_i denotes the power constraint of i^{th} BS.

It is difficult to obtain a closed-form solution to the optimization problem in (38). Therefore, we perform an iterative approach similar to [19]. In particular, the algorithm is initialized by computing $\tilde{\boldsymbol{x}} = (\tilde{\boldsymbol{x}}_1, \tilde{\boldsymbol{x}}_2, \cdots, \tilde{\boldsymbol{x}}_Q)^{\top} = \boldsymbol{H}^{\mathrm{H}}(\boldsymbol{H}\boldsymbol{H}^{\mathrm{H}})^{-1}\boldsymbol{d}$ where $\boldsymbol{d} = \boldsymbol{u} + \tau\boldsymbol{v}^{\star}$ and $\boldsymbol{v}^{\star} = \underset{\hat{\boldsymbol{v}}\in\mathbb{C}}{\text{minimize}}\|\boldsymbol{H}^{\mathrm{H}}(\boldsymbol{H}\boldsymbol{H}^{\mathrm{H}})^{-1}(\boldsymbol{u} + \tau\hat{\boldsymbol{v}})\|$ and the power scaling factor by $\gamma = \max(\{\|\tilde{\boldsymbol{x}}_i\|, i = 1,\cdots,Q\})$.

The iterative processing consist of a nested loop. The inner loop computes $\boldsymbol{x}$ for given $\boldsymbol{v}$ under individual BS power constraint. Since the objective function $\Xi(\boldsymbol{x},\boldsymbol{v},\gamma)$ in (37) is a convex function for a given $\boldsymbol{v}$, we use CVX software [37] to solve for $\boldsymbol{x}$. The outer loop is updated by searching for $\boldsymbol{v}$ in a smaller search radius using sphere encoder [3], [19]. If no new $\boldsymbol{v}$ is found for the reduced search radius, the algorithm is terminated. Pseudo code of our implementation of the algorithm is provided in Algorithm 1. Observe that, $\gamma(n)$ is computed by taking the derivative of (37). In Section V, $\epsilon = 0.001$ is used for illustrative examples.

Algorithm 1: JP MMSE-VP With per BS Power Constraint

repeat
  $n = n + 1, m = 0$
  repeat
    $m = m + 1$
    $\tilde{\gamma}(m) = \frac{\mathrm{Re}(\boldsymbol{d}^{\mathrm{H}}(n-1)\boldsymbol{H}\boldsymbol{x}(m-1))}{\boldsymbol{x}(m-1)^{\mathrm{H}}\boldsymbol{H}^{\mathrm{H}}\boldsymbol{H}\boldsymbol{x}(m-1)+KQN_0}$
    Find $\boldsymbol{x}(m)$ by:

$$\underset{\boldsymbol{x}}{\text{minimize}} \ \|\tilde{\gamma}(m)\boldsymbol{H}\boldsymbol{x} - \boldsymbol{d}(n-1)\|$$
$$\text{subject to } \boldsymbol{x}^{\mathrm{H}}\Pi_i^{\mathrm{H}}\boldsymbol{\Pi}_i\boldsymbol{x} \le P_i, i = 1, 2, \cdots, Q$$

  until $\|\boldsymbol{x}(m) - \boldsymbol{x}(m-1)\|^2 \le \epsilon$
  $\gamma(n) = \frac{\mathrm{Re}(\boldsymbol{d}^{\mathrm{H}}(n-1)\boldsymbol{H}\boldsymbol{x}(m))}{\boldsymbol{x}(m)^{\mathrm{H}}\boldsymbol{H}^{\mathrm{H}}\boldsymbol{H}\boldsymbol{x}(m)+KQN_0}$
  $\mathrm{MSE}(n) = \|\gamma(n)\boldsymbol{H}\boldsymbol{x}(m) - \boldsymbol{d}(n-1)\|^2 + \gamma^2 KQN_0$
  $R(n) = \frac{1}{\tau}\sqrt{\frac{\rho}{KQ}\mathrm{MSE}(n)}$
  Find $\boldsymbol{v}(n)$ within $R(n)$ such that
  $\boldsymbol{v}(n) = \underset{\acute{\boldsymbol{v}}}{\text{minimize}} \|\boldsymbol{H}^{\mathrm{H}}(\boldsymbol{H}\boldsymbol{H}^{\mathrm{H}})^{-1}(\boldsymbol{u} + \tau\acute{\boldsymbol{v}})\|$
  $\boldsymbol{d}(n) = \boldsymbol{u} + \tau\boldsymbol{v}(n)$
until $\boldsymbol{v}(n) \ne \boldsymbol{v}(n-1)$

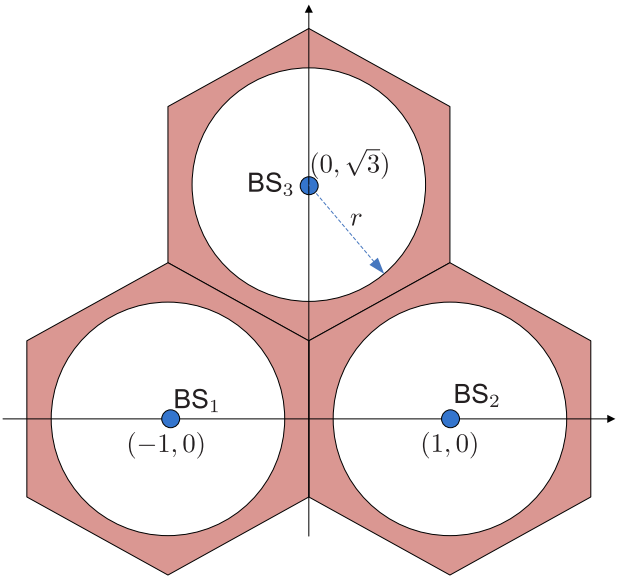

FIGURE 2. Multi-cell downlink transmission - Simulation setup.

V. ILLUSTRATIVE RESULTS

As shown in Fig. 2, we consider a three-cell multi-user CoMP downlink system where the propagation is Rayleigh fading with path-loss exponent α. Therefore, channel coefficients are complex Gaussian with zero mean and variance $r^{-\alpha}$, i.e., $\sim \mathcal{CN}(0, r^{-\alpha})$. Each cell radius is normalized to 1 and the users are uniformly distributed on the radius $0 < r \le 1$ distance from BSs, as shown in Fig. 2. The average BER of a user is investigated.

First, a system where 3 BSs ($Q = 3$) each having 12 transmit antennas ($M = 12$) and each BS serving 4 users ($K = 4$) is considered. Observe that the parameter values satisfy $M = KQ$ and therefore, Schemes 1-5 are feasible. The computational complexity of the selected parameters is provided in Section III-E. The complexity in terms of backhaul overhead is the same for Schemes 1-5 where only CSI and user data local to serving BS is needed. On the other hand, CSI and user data to all the users in the system are assumed available to a central processing unit for the JP MMSE-VP scheme as discussed in Section IV.

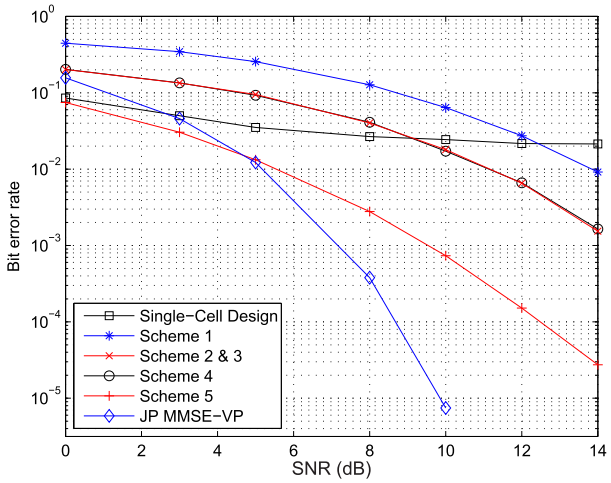

FIGURE 3. BER performance over SNR ($Q = 3$, $M = 12$, $K = 4$, $r = 0.95$, $\alpha = 3$, QPSK).

The BER performance of Schemes 1-5 is shown in Fig. 3. For comparison, the performance of JP MMSE-VP and single-cell MMSE-VP precoder design, i.e., $\boldsymbol{W}_i = \gamma_i \boldsymbol{H}_{ii}^{\mathrm{H}}(\boldsymbol{H}_{ii}\boldsymbol{H}_{ii}^{\mathrm{H}} + \frac{K}{\rho_i}\boldsymbol{I})^{-1}$, $\boldsymbol{G}_i = \boldsymbol{I}$ with $\boldsymbol{v}_i^{\star} = \underset{\acute{\boldsymbol{v}}}{\text{minimize}} \|\boldsymbol{L}_i(\boldsymbol{u} + \tau\acute{\boldsymbol{v}})\|$ where $\boldsymbol{L}_i^{\mathrm{H}}\boldsymbol{L}_i = (\boldsymbol{H}_{ii}\boldsymbol{H}_{ii}^{\mathrm{H}} + \frac{K}{\rho_i}\boldsymbol{I})^{-1}$, is also shown. When the precoder designed for a single-cell is applied in multi-cell settings, a very high error floor is observed owing to the ICI. This observation motivates one to manage the ICI through cooperation. The observed error floor effect has been eliminated by all proposed Schemes 1-5. The proposed IN based Schemes 2 and 3, IA based Scheme 4 and total leakage interference plus MSE minimization based Scheme 5 outperform Scheme 1 in [4]. It is because, Schemes 2-5 exploit advantages of MMSE-VP while Scheme 1 is based on ZF technique. Furthermore, Schemes 2-4 demonstrate a similar performance. It is because, the same DoF is available to serve the intra-cell users after canceling the ICI. Observe that, for the selected parameters, interference is aligned to zero eigenvalue directions and therefore, Scheme 4 also fully suppresses the ICI similar to Schemes 2 and 3. More importantly, Scheme 5 outperforms Schemes 1-4. However, JP MMSE-VP outperforms Scheme 5, especially in smaller BER region. For example, at 10^{-3} BER, Scheme 5 needs 2.4 dB (in SNR) than JP MMSE-VP. These gains achieved by JP MMSE-VP is a result of central-processing in high-dimensional signal

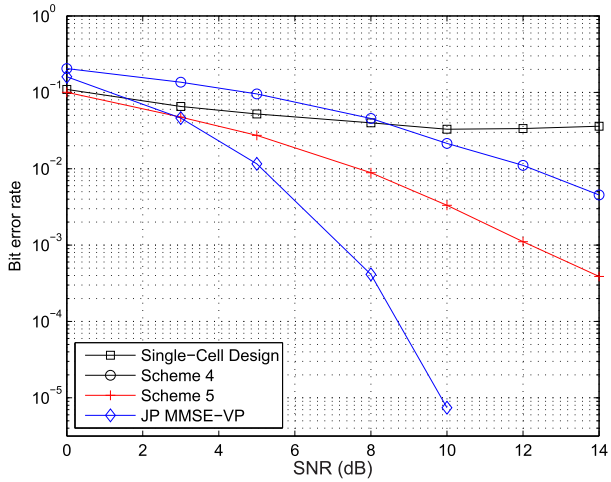

FIGURE 4. BER performance over SNR ($Q = 3$, $M = 10$, $K = 4$, $r = 0.95$, $\alpha = 3$, QPSK).

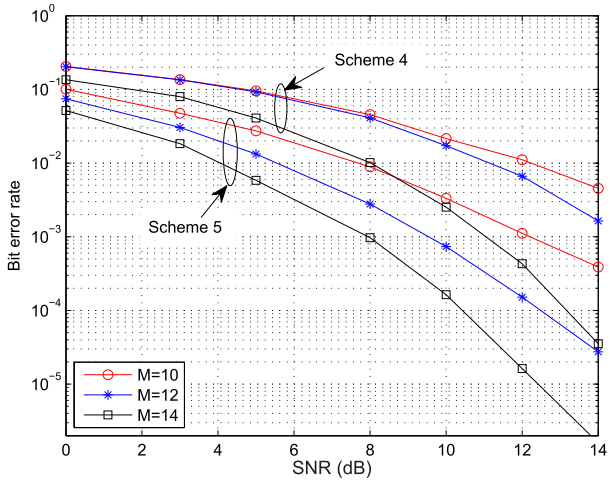

FIGURE 5. BER performance over SNR ($Q = 3$, $M = 10, 12, 14$, $K = 4$, $r = 0.95$, $\alpha = 3$, QPSK).

space for constructive addition of other-cell transmissions rather than treating them as harmful interference. Note that such performance enhancement is feasible with extensive user-data and downlink CSI sharing among BSs at the expense of backhaul overhead and significant infrastructure modifications.

We next study the proposed system performance when $M < KQ$. As a result, Schemes 4 and 5 are feasible while Schemes 1-3 fail. In Fig. 4, we show the performance of Schemes 4 and 5 for $M = 10$, $K = 4$ and $Q = 3$ along with JP MMSE-VP and single-cell design for comparison. Observe from (19) that in IA design, eigenvectors correspond to non-zero eigenvalues has been chosen for precoding. While Scheme 4 is outperformed by Scheme 5, as compared to JP MMSE-VP, Scheme 5 needs a 5.0 dB higher SNR to reach 10^{-3} BER. We observe that Scheme 5 with $M = 12$ (in Fig. 3) has a 2.6 dB SNR gain compared to that with $M = 10$ (in Fig. 4) at 10^{-3} BER.

In Fig. 5, we investigate the impact of increasing M to the BER for Schemes 4 and 5. This scenario is applicable for

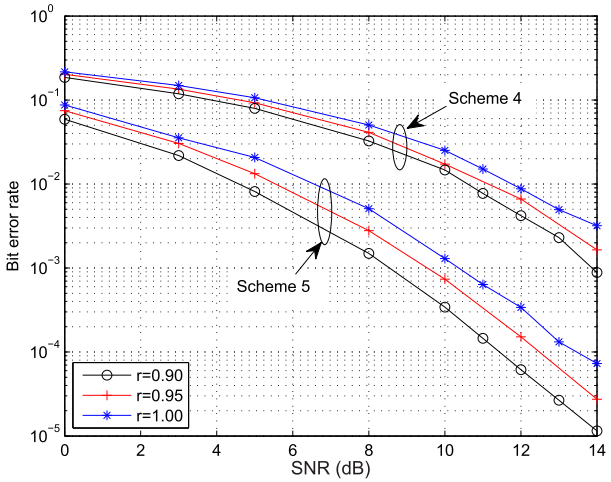

FIGURE 6. BER performance over SNR ($Q = 3$, $M = 12$, $K = 4$, $r = 0.90, 0.95, 1.00$, $\alpha = 3$, QPSK).

large antenna systems. In particular, the BER performance for $M = 10, 12, 14$ when $Q = 3$, $K = 4$ is considered. Observe that at 10^{-3} BER, using $M = 12$ in Scheme 5 gives a 2.6 dB SNR gain compared to $M = 10$ while the gain is as high as 4.3 dB for $M = 14$ compared to $M = 10$.

Next, we study the BER performance over r for Schemes 4 and 5. In particular, Fig. 6 shows the BER performance for $r = 0.90, 0.95, 1.00$ when $M = 12$, $Q = 3$ and $K = 4$. While a user at cell-edge requires higher SNR, numerical results show that, under Scheme 5, a user at $r = 0.95$ requires about 1.0 dB higher SNR to achieve 10^{-3} BER as compared to a user at $r = 0.90$. These results in Figs. 3-6 show that the intra-cell MSE plus total leakage based design is preferred over IN and IA based designs. Therefore, when only local CSI is available to the BS, the DoF available through multiple-antennas can be utilized better by focusing on a balance between intra-cell users' MSE and the ICI.

VI. CONCLUSION

In this paper, interference coordination based non-linear VP precoding for a CoMP downlink transmission is considered. A cascade precoder structure is proposed where an outer precoder mitigates the impact of ICI while the inner precoder utilizes MMSE-VP precoding to provide a high performance intra-cell multi-user transmission. We first consider the trade-off of the DoF available through multiple antennas to mitigate the ICI through the IN and IA techniques. In IN technique that completely eliminates the ICI, we consider the QR and SVD decomposition based outer precoding (i.e., Schemes 2 and 3) which achieves better performance compared to the existing ZF based method (i.e., Scheme 1). To relax the stringent requirement for large antenna arrays in the IN technique, total leakage minimization based IA is proposed for the outer precoding (i.e., Scheme 4). To achieve a closer performance to the JP scheme, the total leakage interference plus intra-cell MSE minimization based precoder (i.e., Scheme 5) is then proposed. Numerical results indicate that utilizing the DoF

available to jointly minimize the total leakage interference plus intra-cell MSE is more beneficial in comparison to total ICI elimination or alignment.

REFERENCES

[1] D. Lee *et al.*, "Coordinated multipoint transmission and reception in LTE-advanced: Deployment scenarios and operational challenges," *IEEE Commun. Mag.*, vol. 50, no. 2, pp. 148–155, Feb. 2012.

[2] M. Sawahashi, Y. Kishiyama, A. Morimoto, D. Nishikawa, and M. Tanno, "Coordinated multipoint transmission/reception techniques for LTE-advanced [coordinated and distributed MIMO]," *IEEE Wireless Commun.*, vol. 17, no. 3, pp. 26–34, Jun. 2010.

[3] M. Mazrouei-Sebdani and W. A. Krzymien, "Vector perturbation precoding for network MIMO: Sum rate, fair user scheduling, and impact of Backhaul delay," *IEEE Trans. Veh. Technol.*, vol. 61, no. 9, pp. 3946–3957, Nov. 2012.

[4] J. Choi, "Multiuser precoding with limited cooperation for large-scale MIMO multicell downlink," *IEEE Trans. Wireless Commun.*, vol. 14, no. 3, pp. 1295–1308, Mar. 2015.

[5] J. G. Andrews, W. Choi, and R. W. Heath, "Overcoming interference in spatial multiplexing MIMO cellular networks," *IEEE Trans. Wireless Commun.*, vol. 14, no. 6, pp. 95–104, Dec. 2007.

[6] D. H. N. Nguyen and T. Le-Ngoc, *Wireless Coordinated Multicell Systems: Architectures and Precoding Designs*. New York, NY, USA: Springer-Verlag, 2014.

[7] M. K. Karakayali, G. J. Foschini, and R. A. Valenzuela, "Network coordination for spectrally efficient communications in cellular systems," *IEEE Wireless Commun.*, vol. 13, no. 4, pp. 56–61, Aug. 2006.

[8] S. Jing, D. N. C. Tse, J. B. Soriaga, J. Hou, J. E. Smee, and R. Padovani, "Downlink macro-diversity in cellular networks," in *Proc. IEEE Int. Symp. Inf. Theory*, Jun. 2007, pp. 1–5.

[9] H. Park, S.-H. Park, H.-B. Kong, and I. Lee, "Weighted sum MSE minimization under per-BS power constraint for network MIMO systems," *IEEE Commun. Lett.*, vol. 16, no. 3, pp. 360–363, Mar. 2012.

[10] Q. H. Spencer, A. L. Swindlehurst, and M. Haardt, "Zero-forcing methods for downlink spatial multiplexing in multiuser MIMO channels," *IEEE Trans. Signal Process.*, vol. 52, no. 2, pp. 461–471, Feb. 2004.

[11] T. M. Kim, F. Sun, and A. J. Paulraj, "Low-complexity MMSE precoding for coordinated multipoint with per-antenna power constraint," *IEEE Signal Process. Lett.*, vol. 20, no. 4, pp. 395–398, Apr. 2013.

[12] T. Zhang, X. Shen, L. Cuthbert, L. Xiao, and C. Feng, "Vector perturbation based adaptive distributed precoding scheme with limited feedback for CoMP systems," *EURASIP J. Wireless Commun. Netw.*, vol. 2011, no. 1, pp. 1–8, Dec. 2011. [Online]. Available: http://dx.doi.org/10.1186/1687-1499-2011-8

[13] D. H. N. Nguyen and T. Le-Ngoc, "Sum-rate maximization in the multicell MIMO broadcast channel with interference coordination," *IEEE Trans. Signal Process.*, vol. 62, no. 6, pp. 1501–1513, Mar. 2014.

[14] D. H. N. Nguyen, H. Nguyen-Le, and T. Le-Ngoc, "Block-diagonalization precoding in a multiuser multicell MIMO system: Competition and coordination," *IEEE Trans. Wireless Commun.*, vol. 13, no. 2, pp. 968–981, Feb. 2014.

[15] G. Caire and S. Shamai (Shitz), "On the achievable throughput of a multiantenna Gaussian broadcast channel," *IEEE Trans. Inf. Theory*, vol. 49, no. 7, pp. 1691–1706, Jul. 2003.

[16] P. Viswanath and D. N. C. Tse, "Sum capacity of the vector Gaussian broadcast channel and uplink-downlink duality," *IEEE Trans. Inf. Theory*, vol. 49, no. 8, pp. 1912–1921, Aug. 2003.

[17] D. J. Ryan, I. B. Collings, I. V. L. Clarkson, and R. W. Heath, "Performance of vector perturbation multiuser MIMO systems with limited feedback," *IEEE Trans. Commun.*, vol. 57, no. 9, pp. 2633–2644, Sep. 2009.

[18] B. M. Hochwald, C. B. Peel, and A. L. Swindlehurst, "A vector-perturbation technique for near-capacity multiantenna multiuser communication—Part II: Perturbation," *IEEE Trans. Commun.*, vol. 53, no. 3, pp. 537–544, Mar. 2005.

[19] M. Mazrouei-Sebdani and W. A. Krzymien, "On MMSE vector-perturbation precoding for MIMO broadcast channels with per-antenna-group power constraints," *IEEE Trans. Signal Process.*, vol. 61, no. 15, pp. 3745–3751, Aug. 2013.

[20] D. A. Schmidt, M. Joham, and W. Utschick, "Minimum mean square error vector precoding," *Eur. Trans. Telecommun.*, vol. 19, no. 3, pp. 219–231, Apr. 2008.

[21] P. Lu and H.-C. Yang, "Vector perturbation precoding for MIMO broadcast channel with quantized channel feedback," in *Proc. IEEE Global Telecommun. Conf.*, Nov./Dec. 2009, pp. 1–5.

[22] C.-B. Chae, S. Shim, and R. W. Heath, "Block diagonalized vector perturbation for multiuser MIMO systems," *IEEE Trans. Wireless Commun.*, vol. 7, no. 11, pp. 4051–4057, Nov. 2008.

[23] A. Razi, D. J. Ryan, I. B. Collings, and J. Yuan, "Sum rates, rate allocation, and user scheduling for multi-user MIMO vector perturbation precoding," *IEEE Trans. Wireless Commun.*, vol. 9, no. 1, pp. 356–365, Jan. 2010.

[24] J. Maurer, J. Jaldén, D. Seethaler, and G. Matz, "Vector perturbation precoding revisited," *IEEE Trans. Signal Process.*, vol. 59, no. 1, pp. 315–328, Jan. 2011.

[25] R. Chen, C. Li, J. Li, and Y. Zhang, "Low complexity user grouping vector perturbation," *IEEE Wireless Commun. Lett.*, vol. 1, no. 3, pp. 189–192, Jun. 2012.

[26] S. P. Herath, D. H. N. Nguyen, and T. Le-Ngoc, "Vector-perturbation precoding under quantized CSI," *IEEE Trans. Veh. Technol.*, Early access article.

[27] J. Park, B. Lee, and B. Shim, "A MMSE vector precoding with block diagonalization for multiuser MIMO downlink," *IEEE Trans. Commun.*, vol. 60, no. 2, pp. 569–577, Feb. 2012.

[28] S. W. Peters and R. W. Heath, "Cooperative algorithms for MIMO interference channels," *IEEE Trans. Veh. Technol.*, vol. 60, no. 1, pp. 206–218, Jan. 2011.

[29] K. Gomadam, V. R. Cadambe, and S. A. Jafar, "Approaching the capacity of wireless networks through distributed interference alignment," in *Proc. IEEE Global Telecommun. Conf.*, Nov./Dec. 2008, pp. 1–6.

[30] B. Lee and B. Shim, "A vector perturbation with user selection for multiuser MIMO downlink," *IEEE Trans. Commun.*, vol. 60, no. 11, pp. 3322–3331, Nov. 2012.

[31] C. Masouros, M. Sellathurai, and T. Ratnarajah, "Computationally efficient vector perturbation precoding using thresholded optimization," *IEEE Trans. Commun.*, vol. 61, no. 5, pp. 1880–1890, May 2013.

[32] V. R. Cadambe and S. A. Jafar, "Interference alignment and degrees of freedom of the K-user interference channel," *IEEE Trans. Inf. Theory*, vol. 54, no. 8, pp. 3425–3441, Aug. 2008.

[33] M. A. Maddah-Ali, A. S. Motahari, and A. K. Khandani, "Communication over MIMO X channels: Interference alignment, decomposition, and performance analysis," *IEEE Trans. Inf. Theory*, vol. 54, no. 8, pp. 3457–3470, Aug. 2008.

[34] H. Lütkepohl, *Handbook of Matrices*. New York, NY, USA: Wiley, 1997.

[35] K. B. Petersen and M. S. Pedersen, *The Matrix Cookbook*. Lyngby, Denmark: Technical Univ. Denmark, Nov. 2008.

[36] F. Sun and E. de Carvalho, "A leakage-based MMSE beamforming design for a MIMO interference channel," *IEEE Signal Process. Lett.*, vol. 19, no. 6, pp. 368–371, Jun. 2012.

[37] CVX Research, Inc. (Mar. 2014). *CVX: MATLAB Software for Disciplined Convex Programming, Version 2.1*. [Online]. Available: http://cvxr.com/cvx

SANJEEWA P. HERATH (S'09) received the B.Sc. (Hons.) degree in electronics and telecommunication engineering from the University of Moratuwa, Moratuwa, Sri Lanka, in 2005, and the M.Eng. (Thesis) degree in telecommunications from the Asian Institute of Technology, Pathumthani, Thailand, in 2009. He is currently pursuing the Ph.D. degree with the Department of Electrical and Computer Engineering, McGill University, Montréal, QC, Canada.

He was a Software Engineer with Millennium IT Software (Pvt) Ltd., and a member of the London Stock Exchange Group, where he designed and developed capital markets exchange system related modules (2005–2009). His current research interest is in the areas of multiuser communication and multiple-antenna systems.

Mr. Herath was a recipient of the A.B. Sharma Memorial Prize from the Asian Institute of Technology in recognition to having the best thesis in the fields of information and communication technologies and telecommunications, in 2009.

DUY H. N. NGUYEN (S'07–M'14) received the B.Eng. (Hons.) degree from the Swinburne University of Technology, Hawthorn, VIC, Australia, in 2005, the M.Sc. degree from the University of Saskatchewan, Saskatoon, SK, Canada, in 2009, and the Ph.D. degree from McGill University, Montréal, QC, Canada, in 2013, all in electrical engineering. Since 2013, he has been a Research Associate with the Department of Electrical and Computer Engineering, McGill University, and a Post-Doctoral Research Fellow with the Institut National de la Recherche Scientifique, Université du Québec, Montréal. His research interests include resource allocation in wireless networks, signal processing for communications, convex optimization, and game theory.

Dr. Nguyen was a recipient of the Australian Development Scholarship for his undergraduate study in Australia, the McGill Engineering Doctoral Award, and the Fonds de recherche du Québec–Nature et technologies (FRQNT) Doctoral Fellowship. Since 2013, he has been a recipient of the FRQNT Post-Doctoral Fellowship.

THO LE-NGOC (F'97) received the B.Eng. (Hons.) degree in electrical engineering in 1976, the M.Eng. degree from McGill University, Montreal, in 1978, and the Ph.D. degree in digital communications from the University of Ottawa, Canada, in 1983. From 1977 to 1982, he was with Spar Aerospace Ltd., and involved in the development and design of satellite communications systems. From 1982 to 1985, he was an Engineering Manager of the Radio Group with the Department of Development Engineering, SRTelecom Inc., where he developed the new point-to-multipoint DA-TDMA/TDM Subscriber Radio System SR500. From 1985 to 2000, he was a Professor with the Department of Electrical and Computer Engineering, Concordia University. Since 2000, he has been with the Department of Electrical and Computer Engineering, McGill University. His research interest is in the area of broadband digital communications. He is a fellow of the Engineering Institute of Canada, the Canadian Academy of Engineering, and the Royal Society of Canada. He was a recipient of the Canadian Award in Telecommunications Research 2004, and the IEEE Canada Fessenden Award 2005. He holds a Canada Research Chair (Tier I) on Broadband Access Communications.